BIOPHYSICAL CHEMISTRY 1 (1974) 184–203. © NORTH-HOLLAND PUBLISHING COMPANY

PHYSICAL CHEMICAL STUDIES OF SHORT-CHAIN LECITHIN HOMOLOGUES. II. MICELLAR WEIGHTS OF DIHEXANOYL- AND DIHEPTANOYLLECITHIN

R.J.M. TAUSK, J. VAN ESCH, J. KARMIGGELT, G. VOORDOUW and J.Th.G. OVERBEEK
Van 't Hoff Laboratory, State University, Utrecht, The Netherlands

Received 2 August 1973

The micellar weights of dihexanoyl- and diheptanoyllecithin in aqueous solutions are calculated from light scattering and ultracentrifugation data. A monomer–micelle assocation model is used and corrections for the thermodynamic nonideality, on the basis of rigid noninteracting particles, are applied. A few experiments on the influence of high NaCl concentrations (up to 3 M) are described. Dihexanoyllecithin forms micelles with micellar weight of 15 000 to 20 000 and with rather narrow weight distributions. Diheptanoyllecithin micelles however, have broad size distributions with micellar weights of 20 000 up to about 100 000 in the concentration range studied. Micelles are assumed to be spherical or to have sphero-cylindrical shapes depending on the molecular weights. Two models are used: (1) a compact structure, where no attention is paid to the hydrocarbon–water contact (2) micelles with as little hydrocarbon–water contact as possible.

1. Introduction

In the first paper of this series [1] we outlined the importance of the knowledge of the aggregation properties of short-chain lecithins for the understanding of certain biochemical processes. In one of these processes, the enzymatic hydrolysis of lecithins by phospholipase A [2], it appeared that the kinetics are profoundly influenced by the micellar structure.

In this paper we describe micellar weight determinations of dihexanoyl- and diheptanoyllecithin, performed by light scattering and analytical ultracentrifugation. In order to estimate the micellar weight distribution the thermodynamic nonideality of the solutions has to be taken into account. The second virial coefficients will be discussed in some detail on the basis of the excluded volume of rigid noninteracting molecules.

2. Methods and materials

The preparation and purification of dihexanoyl- and diheptanoyllecithin as well as the preparation of the aqueous solutions, containing 10^{-2}M phosphate buffer (pH = 6.9 ± 0.1) and variable concentrations of NaCl have been described in part I of this series [1]. In all mass per unit volume concentrations we assume the lecithin to be present as monohydrate.

2.1. Ultracentrifugation

Low speed sedimentation–diffusion equilibrium experiments [3] were performed with Beckman Spinco E analytical ultracentrifuges, equipped with Rayleigh- and Schlieren optics and RTIC units. The optical parts were aligned according to the procedure of Brinkhuis et al. [4]. The photographs of the Rayleigh interference pattern were read on a comparator (Aus Jena). The photographs of the Schlieren pattern were enlarged photographically and redrawn. The resulting curves were graphically smoothed. The aluminum, Kel F or Al-filled epon cells contained an oil layer (FC-43), which we added after it was shown that this oil did not disturb the micellar equilibrium. Experiments were performed at 24 ± 1°C. The individual runs for diC_6- and diC_7-lecithin took about 20 hours and 40 hours respectively.

2.2. Light scattering

Two light scattering instruments, manufactured by the Société Française d'Instruments de Contrôle et d'Analyses, were used. The measurements on diC_6-lecithin were performed with the Sofica Photo-Gonio-Diffusomètre model 40 000 B, which had been modified by Huisman [5]. Experiments on diC_7-lecithin were done with the Fica 50.

The solutions were filtered, mostly under pressure, through millipore filters (50 nm or 20 nm) directly into measuring cells [5]. The cells were then centrifuged in a Beckman preparative centrifuge (Model Spinco L) at 20 000 rpm, while floating in a mixture of carbontetrachloride and petroleum ether or in nearly saturated aqueous solutions of sodium nitrate. This last solution is preferable since organic vapors are easily solubilized in the micelles.

2.3. Refractive index increments

The refractive index increments were measured with a Rayleigh interferometer (Aus Jena) at $\lambda = 546$ nm and at room temperature (22 ± 1°C). When experiments were performed in aqueous solutions containing high concentrations of NaCl, the cell walls were first treated with dichloro-dimethylsilane to render the glass hydrophobic and prevent creeping of the salt.

2.4. Density measurement

The densities of the aqueous lecithin solutions were measured with the digital density measuring device DMA-02/C from Anton Paar (Graz) [6]. The system was checked with KCl solutions [7] and the experiments were performed at 25°. During every dilution series temperature stability was about ± 0.003°C. Reproducibility was within $\pm 3 \times 10^{-6}$ g ml^{-1}.

2.5. Vapor pressure osmometry

A few molecular weight measurements by vapor pressure osmometry were performed on diC_6-lecithin using the Hitachi Perkin Elmer Molecular Weight Apparatus Model 115 at 48.5°C and 60°C. The lecithin was dissolved in pure water or in 10^{-4}M phosphate buffer. The osmometer was calibrated with mannitol and sucrose. In the concentration range of 5×10^{-3}–1.5×10^{-1} M sugar reproducibilities of 0.2–0.5% were achieved.

3. Light scattering and ultracentrifugation equations

In order to interpret the measurements in terms of an association process we assume the lecithin to be composed of several species: monomers and several types of micelles with different micellar aggregation numbers. We start from multicomponent light scattering or ultracentrifugation equations and relate the concentrations of the different lecithin components (species) to each other by association constants afterwards. Thermodynamically lecithin is of course only one component.

One of the equations used [8–12] for the light scattered by a solution in excess over the solvent scattering for a multicomponent system composed of isotropic particles with dimensions and interaction distances small compared to the wavelength is

$$\frac{K'c}{R_{90}} = \frac{1}{\sum_i f_i M_i n_i^2} + c \frac{\sum_i \sum_j f_i f_j n_i n_j A_{ij}}{(\sum_i f_i M_i n_i^2)^2} + \ldots\ldots\ldots \quad (1)$$

where K' stands for the constant $2\pi^2 n_0^2 \lambda_v^{-4} N_0^{-1}$, n_0 is the refractive index of the solvent, λ_v is the wavelength in vacuum and N_0 is Avogadro's constant. R_{90} stands for the excess Rayleigh ratio at an angle perpendicular to the incident beam ($R_{90} = (3/16\pi) \times$ turbidity) and c is the total concentration in mass per unit volume ($c = \Sigma_i c_i$). f_i equals the weight fraction ($= c_i/c$) of a solute component i, with molecular weight M_i and refractive index increment n_i

$$n_i = (\partial n/\partial c_i)_{P,T,c'} \quad (2)$$

This differentiation is performed at constant pressure, temperature and concentrations of all solute components except i. The summations in eq. (1) are performed over all solute components i and j. For an incompressible solution the interaction parameter A_{ij} is found from the change of the activity coefficient γ_i of component i with the concentration of component j.

$$A_{ij} = (\partial \ln \gamma_i/\partial C_j)_{\mu_0,T,C'} \quad (3)$$

The differentiation to concentration C_j (in amount per unit volume) is performed at constant temperature, concentrations of solute components (except j) and chemical potential of the solvent (μ_0). The activity coefficient γ_i stems from the chemical potential of solute component i according to

$$\mu_i = \mu_i^0(\mu_0, T, C') + RT \ln C_i\gamma_i. \tag{4}$$

The ultracentrifugation equilibrium equation reads [12, 13]

$$\left(\frac{RT}{\omega^2 rc}\frac{dc}{dr}\right)^{-1} = \frac{1}{\sum_i f_i M_i \rho_i} + c\,\frac{\sum_i\sum_j f_i f_j \rho_j A_{ij}}{(\sum_i f_i M_i \rho_i)^2}. \tag{5}$$

R and T are the gas constant and the absolute temperature respectively, ω is the angular velocity and ρ_i equals the density increment

$$\rho_i = (\partial\rho/\partial c_i)_{P,T,c'}. \tag{6}$$

All other symbols in eq. (5) have the same meaning as in eq. (1). The measured quantities $R_{90}/K'c$ and $(RT/\omega^2 rc)$ (dc/dr) will be called the *reduced total apparent weight average molecular weights:* $\langle M(\partial n/\partial c)^2\rangle_{w.app.}$ or $\langle M(\partial\rho/\partial c)\rangle_{w.app.}$.

It is impossible to distinguish between association and thermodynamic nonideality from thermodynamic data alone. This means that one can only get detailed information about the association phenomenon after accepting a model for the nonideality. In order to calculate the real weight average molecular weight $\langle M\rangle_{w.id.} = \Sigma_i f_i M_i$ from measured quantities we will have to estimate:

(1) The second terms on the right hand side of eqs. (1) and (5). To obtain these virial terms we need estimates of (i) the interaction parameter A_{ij}, and (ii) the weight fractions f_i of the different lecithin species. Both subjects will be discussed in section 6.

(2) The mean density increment or the refractive index increment squared. These are a kind of Z-averages as can be seen from the following relation

$$\langle\partial\rho/\partial c\rangle_z = \sum_i f_i M_i \rho_i / \sum_i f_i M_i, \tag{7}$$

a further interpretation of these increments is given in the next section.

From the total average molecular weight and the monomer concentration the micellar weight can be obtained. Relations for estimating the monomer concentration are also given in the next section.

4. Association equilibrium

In this section we assume all lecithin species to be in equilibrium with one another. This implies that relations between the concentrations (or activities) of the various species exist.

An impression of the micellar weight distribution can be obtained if the weight and number average micellar weights $[\langle M\rangle_{n.id.mic.} = (\Sigma_{i=2} f_i/M_i)^{-1}]$ are known. The lecithin species are denoted with a subscript i, whose value equals the association number.

If the chemical potential of a species is given by the relation

$$\mu_i = \mu_i^0(P, T, c') + RT \ln a_i$$
$$= \mu_i^0 + RT\,[\ln c_i + M_i(B_1 c + B_2 c^2 + \ldots)], \tag{8}$$

in which a_i is the activity of a solute species i, and B_1, B_2, etc., are independent of i, one can easily prove that the following relation between the concentration of that species and the total concentration holds

$$dc_i/dc = c_i M_i / c\langle M\rangle_{w.id.} \tag{9}$$

Using this equation one readily obtains the well known [14–18] relations for calculating the monomer weight fraction, f_1, and the number average molecular weight from the dependence of the weight average molecular weight on the total concentration

$$\ln f_1 = \int_0^c (M_1/\langle M\rangle_{w.id.} - 1)\, c^{-1}\, dc, \tag{10}$$

and

$$c/\langle M\rangle_{n.id.} = \int_0^c \langle M\rangle_{w.id.}^{-1}\, dc. \tag{11}$$

These equations apply irrespective of the relations between the different association constants between the various associating species.

Other types of averages can also be calculated. The Z-average molecular weight is obtained from

$$\langle M\rangle_{z.id.} = \sum_i f_i M_i^2 / \sum_i f_i M_i = \frac{d}{dc}(c\langle M\rangle_{w.id.}). \tag{12}$$

The Z-average density increment likewise follows from

$$\langle \partial\rho/\partial c\rangle_z = \frac{\mathrm{d}}{\mathrm{d}c}\left[\sum_i c_i(\partial\rho/\partial c_i)_{R,T,c'}\right] = \frac{\partial\rho}{\partial c}. \qquad (13)$$

It can thus be seen that this mean increment, at concentration c, that has to be inserted into eq. (5) equals the measured density increment. The mean refractive index increment squared should be calculated from the definition

$$\langle(\partial n/\partial c)^2\rangle_Z = \sum_i f_i M_i n_i^2 / \sum_i f_i M_i. \qquad (14)$$

Due to the high association numbers in micellar systems the transition at the CMC is rather sharp. At concentrations outside the small transition region the Z-average increments become indistinguishable from the limiting values for monomers and micelles.

The equations given above apply only for systems at constant pressure. In ultracentrifugation, however, pressure is not constant in the cell and varies from one experiment to the other. For each separate experiment eqs. (9–12) do hold for systems in which the partial specific volume of each species is concentration independent, if the reduced molecular weights (thus including the factor $\partial\rho/\partial c$) are substituted.

If apparent weight average molecular weights are used eq. (11) yields the apparent number average molecular weight and eqs. (10) and (9) provide us with the first estimates of the true activities a_1 or a_i (defined with the help of eq. (8).

In general relation (8), however, does not apply [8, 10]. Using classic thermodynamics one can derive for an incompressible system the relation (15) between the chemical potentials and the coefficients $A_{\bar{i}}$ introduced in eq. (3).

$$\mu_i = \mu_i^0(P,T,c') + RT\ln c_i + RT\sum_j M_j^{-1}(A_{\bar{i}\bar{j}} - \bar{V}_i)c_j + \ldots\ldots \qquad (15)$$

$\bar{V}_i$ equals the partial molal volume of species i. In section 6 dealing with the *second virial coefficient* a simple model for calculating $A_{\bar{i}\bar{j}}$ will be described. The model is based on rigid non-interacting solute molecules. It has often been realized [19–22], that eq. (15) (neglecting $\bar{V}_i$) reduces to eq. (8) for rigid long cylinders with equal radii. In the case of spherical solute molecules B_1 in eq. (8) is inversely proportional to the molecular weight. It can however be shown that the errors involved in using eq. (9) through (13) are often small, especially in micellar systems.

5. Micellar weight distribution

In the preceding section an equation (11) has been given to obtain the number average from the weight average molecular weight. This equation holds for the total molecular weight and for the micellar weight. The ratio $Q = \langle M\rangle_{\mathrm{w.id.mic.}}/\langle M\rangle_{\mathrm{n.id.mic.}}$ for the real (often called ideal) micellar weights is a measure of the width of the distribution. The standard deviation σ_n around the number average molecular weight for an arbitrary distribution is given by [23]

$$\sigma_n/\langle M\rangle_n = (Q-1)^{1/2}. \qquad (16)$$

The actual weight distribution depends on all association constants, but these are generally unknown unless experiments of extremely high accuracy and a very detailed model of the association behaviour are available.

Wide molecular weight distributions are expected if the association constant K for different micelles are about equal

$$K = C_{n+1}/C_nC_1. \qquad (17)$$

C_n stands for the molar concentration of a micelle containing n monomers. Equal values of K are likely to appear, if the micellar structure strongly departs from the spherical shape and lead to Q values of 2, as has been shown in several papers [18, 21, 24, 25]. This model also leads to a linear increase of the micellar weight with the square root of the micellar concentration.

In the calculations of the second virial coefficients we would like to use actual values for the concentrations of the various micelles. Instead of making assumptions about the various association constants we assume that the Schulz distribution function [13, 26] applies. This is a two parameter function which is easy to integrate. One of the variables can be expressed as $\langle M\rangle_w/\langle M\rangle_n$

$$f(M) = (y^{z+1}/\Gamma_{z+1})M^z\exp[-yM], \qquad (18)$$

where $f(M)$ stands for the weight fraction of the molecules with a molecular weight M;

$y = (z + 1)/\langle M\rangle_w$; $\quad z = \langle M\rangle_n/(\langle M\rangle_w - \langle M\rangle_n)$;

Γ_{z+1} is the gamma function.

6. Second virial coefficient

Details of the micellisation phenomenon can only be obtained after estimation of the coefficients of the second terms on the right hand side of eqs. (1) and (5). These terms contain next to the weight fractions the interaction parameters A_{ij}. Evaluation of this last quantity is actually the basic problem.

6.1. Interaction parameter A_{ij}

As the electrostatic dipole intermicellar interactions are probably quite small one may visualize the micelles as rigid noninteracting particles. A_{ij} is related to the pair correlation function [8, 10] and can in this simplified case be calculated from the mutual pair excluded volume. Isihara solved this problem for molecules of arbitrary size and shape. The relation for A_{ij} (defined in our concentration units) reads

$$A_{ij} = N_0[v_i + v_j + (1/4\pi)(x_i s_j + x_j s_i)], \qquad (19)$$

where v_i stands for the volume of a molecule i with surface s_i, and x_i equals the integral over all orientations ω of H_i, called the supporting function.

$$x_i = \int H_i \, d\omega. \qquad (20)$$

For simplicity's sake we will assume the lecithin monomers to be spheres and the micelles to be spheres or spherocylinders. The geometry of these molecules is given in fig. 1 and the definition of H_i and the relations needed to calculate A_{ij} are given in table 1. If there is a distribution in micellar weights we assume the spherocylinders to have equal radii and different lengths and the spheres to have different radii. These models will be discussed in more detail in section 9.

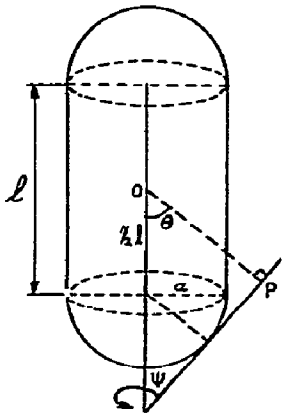

Fig. 1. Geometry of a spherocylinder.

6.2. Weight fractions of the various species

The monomer concentrations and the total micellar concentrations can be evaluated with the help of eq. (10). The weight fractions of the different types of micelles can be estimated from an assigned distribution function. We have assumed the Schulz distribution (eq. (18)) to apply. The two independent parameters in that relation can be obtained from the weight and the number average micellar weight.

It will be important that the value of the second virial coefficient is not too sensitive to the actual applied distribution function. The influence of the width of the distribution can readily be found by solving the second terms of eqs. (1) and (5) for different geometric models (different relations for A_{ij} in eq. (19)) and polydispersities. The virial coefficient for mixtures of spherocylinders with equal radii and weight average molecular weights is independent of the width of the distribution.

Table 1
Size and shape parameters for the calculation of the interaction parameter A_{ij}

	Sphere	Spherocylinder
v	$\frac{4}{3}\pi a^3$	$\frac{4}{3}\pi a^3 + \pi a^2 l$
s	$4\pi a^2$	$4\pi a^2 + 2\pi a l$
H	a	$a + \frac{1}{2} l \cos\theta$
x	$4\pi a$	$4\pi a + \pi l$

For mixtures of spheres with equal partial specific volumes $\bar{v}$ the nonideality coefficient decreases with increasing width. Assigning a value of $8\,M_w\,\bar{v}$ to the total excluded volume of a monodisperse system we find at $M_w/M_n=2$ a volume of $7.39\,M_w\bar{v}$ and at $M_w/M_n=\infty$ a value of $6.84\,M_w\bar{v}$.

7. Procedure for calculating micellar weights

7.1. Light scattering

We will now discuss the actual procedure for calculating the micellar weights from light scattering data. We start from the plot of the reduced total apparent weight average molecular weight ($R_{90}/K'c \equiv \langle M(\partial n/\partial c)^2\rangle_{w.app.}$) versus the total concentration and divide these "molecular weights" by the average refractive index increment squared and obtain the values for $\langle M\rangle_{w.app.}$. The values for $\langle(\partial n/\partial c)^2\rangle_z$ near the CMC are calculated using eq. (14) from estimates of the monomer concentration (eq. (10)), micellar concentrations, association numbers and the refractive index increments measured at concentrations well outside the CMC region.

The values from the resulting curve of $\langle M\rangle_{w.app.}$ versus c are now used in eqs. (10) and (11), since these equations can also be used when substituting apparent values, as stated there. We now arrive at the monomer activity f_{1a}, the apparent weight average micellar weight $\langle M\rangle_{w.app.mic.}$ and the apparent number average micellar weight $\langle M\rangle_{n.app.mic.}$. The following approximation was used:

$$\langle M\rangle_{w.app.mic.} = (\langle M\rangle_{w.app.} - M_1 f_{1a})/(1-f_{1a}). \qquad (21)$$

The values of $\langle M\rangle_{w.app.mic.}$ should provide us with the information necessary to estimate the shapes and sizes of the micelles, while the values for $\langle M\rangle_{w.app.mic.}/\langle M\rangle_{n.app.mic.}$ give us an estimate of the polydispersity of the micelles. Using the Schulz distribution (eq. (18)), the monomer concentration and the values for A_{ij} from geometric models (eq. (19)), the summations in the second virial coefficient of eq. (1) can be carried out. In most cases the summations can be replaced by integrals.

After the reduced total ideal weight average molecular weights are calculated we start micellar weight estimations by again using eqs. (7), (10) and (11). The resulting micellar weights provide us with a better estimate of the second virial coefficient and weight average micellar weights are obtained using a sufficient number of iterations. This whole procedure is schematically given in fig. 2.

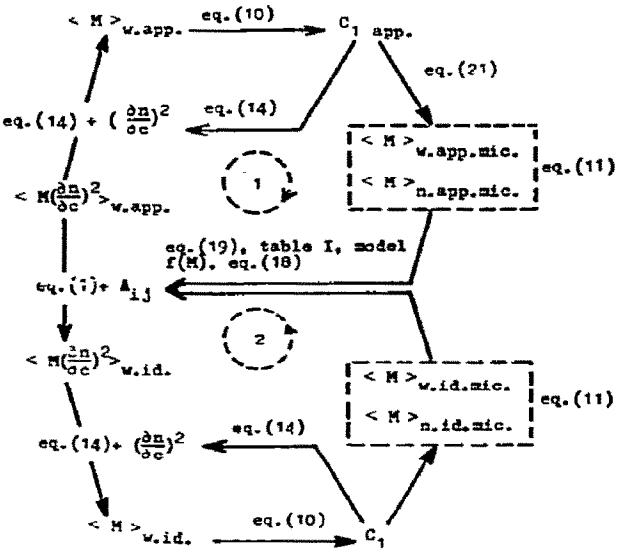

Fig. 2. Procedure for calculating the ideal micellar weights from reduced apparent total weight average molecular weights.

Cycle 1. The apparent weight and number average micellar weights are obtained from the total apparent molecular weights with the help of eqs. (10) and (11). At concentrations near the CMC an iteration procedure is used to calculate $(\partial n/\partial c)$ from eq. (14). From the weight average micellar weights the micellar shape and size is estimated. This leads to the first approximation of the interaction parameter A_{ij} (eq. (19)). The parameters of the distribution function $f(M)$ (eq. (18)) are obtained from a comparison of the number and weight average micellar weights.

Cycle 2. Introduction of the weight fractions, the values of A_{ij} and $(\partial n/\partial c)$ in eq. (1) leads to estimates of the ideal total molecular weights from which the micellar weights are obtained. An iteration procedure provides us with better estimates of A_{ij}.

7.2. Ultracentrifugation

Evaluation with the help of eq. (10) of the micellar weight at a certain concentration above the CMC requires the knowledge of the total average molecular weight at all lower concentrations.

If we want to keep the time to reach equilibrium within reasonable limits we have to use small solution columns (around 3 mm), which allow only a modest concentration range in one experiment. Experiments

with various starting concentrations but with overlapping equilibrium concentration ranges are performed. At the lowest concentrations the highest speeds are required in order to get an optimal resolution.

The hydrostatic pressure in the solution columns therefore varies from one experiment to the other. Since the partial specific volume of monomers and micelles differ the association equilibrium is pressure dependent. This leads to a nonsuperposition of the plots of $\langle M\, \partial\rho/\partial c\rangle_{w,app.}$ against c from different experiments [32]. In this case the micellar weights should be calculated for every experiment separately, but this demands an extremely high accuracy. Moreover, the theoretical pressure effects in our case result in a nonsuperposition of a few percent at most, as follows from some estimated numerical data for diC_6- under our experimental conditions. At the lowest concentration and at the bottom positions in the cells a maximal pressure of 17 atm prevailed. The measured total average molecular weights are smaller than the molecular weights if obtained at 1 atm pressure [32]. At total concentrations of 8 mg ml^{-1}, 11 mg ml^{-1} and 20 mg ml^{-1} the decrease of the molecular weight due to the pressure is only 4%, 2% and 0.5% respectively. The calculated effects for diC_7- are even much smaller. We therefore neglect the pressure effects and plot $\langle M\, \partial\rho/\partial c\rangle_{w,app.}$ values versus c from different experiments on one curve and analyse this curve in a manner completely analogous to the method used in interpreting the light scattering data.

8. Results

8.1. Refractive index increment

The change in the refractive index of the solution with increasing lecithin concentration can be described by two straight lines, intersecting near the CMC. The curvature near the CMC extended only over a very small concentration range. The expression for the refractive index change above the CMC is given by

$$\Delta n = (\partial n/\partial c)_{P,T} c + a, \qquad (22)$$

and we may identify this increment with the micellar refractive index increment $(\partial n/\partial c)_m$. The increment for monomers will be abbreviated with $(\partial n/\partial c)_1$. In table 2 the values of the increments and of the constant a are given for diC_6-lecithin in aqueous solutions containing various NaCl concentrations and for diC_7-lecithin. The value for diC_8-lecithin is also included for comparison. In this special case it is not possible to measure the increment at room temperature in electrolyte free (or dilute buffer) solutions, due to the appearance of a phase separation (to be published).

The decrease of the refractive index increment $(\partial n/\partial c)_s - (\partial n/\partial c)_0$ of the lecithin with increasing salt concentrations can be explained by taking the increase of the refractive index of the medium $n_s - n_0$ into account. Assuming the refractive index of a solution to be a linear function of the volume composition of the various components the following relation holds [12, 33]

$$(\partial n/\partial c)_s - (\partial n/\partial c)_0 = -(n_s - n_0)\bar{v}, \qquad (23)$$

$\bar{v}$ equals the partial specific volume of the lecithin. In table 2 we also give the values for the refractive index increments calculated from this equation, using the partial specific volumes and the refractive index increments both measured in 10^{-2}M phosphate buffer.

8.2. Density measurements

In plotting density values ρ versus lecithin concentrations straight lines intersecting near the CMC were obtained. As in refractive index measurements only a slight curvature near the CMC was found. From the slopes of the lines the partial specific volumes $\bar{v}$ and the partial molal volumes $\overline{V}$ were calculated [12]. The data for diC_6- and diC_7-lecithin are given in table 3.

By subtraction of appropriate values from each other the volume of a mole CH_2 and the volume change during micellisation are found. These values compare favorably with data for other soaps studied by Corkill [34].

In the last column of table 3 we added for comparison the molar volumes calculated from data of longer chain lecithin homologues in the L–α liquid crystalline phase [35–37].

8.3. Vapor pressure osmometry

We only succeeded in measurements of molecular weights by vapor pressure osmometry at concentrations below the CMC for diC_6-lecithin. Up to a concentration of about 6 mg ml^{-1} a molecular weight of 471 ± 2 was

Table 2
Refractive index increments for three lecithin homologues

Lecithin	M NaCl	observed $\partial n/\partial c$ (ml g^{-1})		$a \times 10^6$	$\partial n/\partial c$ [eq. (23)]	
		$c <$ CMC	$c >$ CMC	$c >$ CMC	$c >$ CMC	$c >$ CMC
diC_6-	0	0.132(0.001) [a]	0.126(0.001)	37		
	1	0.122(0.001)	0.113(0.001)	31	0.124	0.118 [d]
	2	0.117(0.002)	0.1073(0.001)	19	0.116	0.110 [d]
	3	0.111(0.002)	0.0997(0.001)	12	0.109	0.102 [d]
diC_7-	0	0.136(0.002)	0.125(0.001)	11		
diC_8-	0 [b]		0.125(0.002)			
	0 [c]		0.118(0.001)			0.119 [e]

[a] The numbers between brackets are the standard deviations from least square straight lines.
[b] This value was obtained by extrapolating measurements from high temperatures (50–90°C).
[c] Measured in solutions containing 0.2 M LiI.
[d] Calculated on the basis of measured values in salt free solutions.
[e] Corrected for the LiI effect from extrapolated measurements at high temperatures (to be published, see also ref. [1]).

obtained, which is in perfect agreement with the monohydrate monomer molecular weight (471.5). This means that there is no substantial preassociation. At higher concentrations measurements were progressively less reliable, probably due to decomposition of the lecithin and the formation of the more volatile caproic acid at the high temperatures: 48.5°C and 60°C. The osmometer signals became unstable and the calibration constant showed sudden jumps, leading to too small apparent molecular weights.

8.4. Calibration of the light scattering instrument

The following systems were used in the calibration.

(a) Lysozyme (Boehringer & Soehne, for analytical purposes). The protein was dissolved in a Na_2HPO_4 (0.056 M) – citric acid (0.071 M) buffer (pH = 3.7) to suppress dimerisation [38]. The molecular weight was found from ultracentrifugation equilibrium experiments and was in agreement with other physical analyses [39] and with the chemical analysis [40].

Table 3
Density increments and molal volumes of dihexanoyl- and diheptanoyllecithin

Lecithin	$\partial\rho/\partial c$		$\bar{V}_2$ (ml $mole^{-1}$)		$\bar{V}_{CH_2}$ (ml $mole^{-1}$)		$\Delta\bar{V}_2$	V_2
	$c <$ CMC	$c >$ CMC	$c <$ CMC	$c >$ CMC	$c <$ CMC	$c >$ CMC	micellisation	L–α
diC_6-	0.1513(0.0007)	0.1324(0.0007)	401.3(0.4)	410.3(0.4)			9.0(0.6)	411.3
diC_7-	0.139 (0.003)	0.1103(0.0005)	431.4(1.5)	445.8(0.3)	15(1.6)	17.7(0.5)	14.4(1.6)	443.8

(b) β-Lactoglobulin*. Crystalline bovine lactoglobulin was dissolved in 10^{-3} M EDTA (pH = 6.0), 0.2 M NaCl and dialyzed for 24 hours. The concentrations were determined by absorption measurements ($E^{1\%}_{278} = 9.1$) [41]. The refractive index increment was taken [41, 42] to be 0.182 ml g^{-1}. The dimer molecular weight [41] was found by ultracentrifugation (36700).

(c) 12-Tungstosilicic acid (Merck, p.a.). The calibration constant from TSA in aqueous solutions containing 0.3 M or 1M NaCl was obtained by extrapolation to infinite dilution. The refractive index increments from literature were used [43] (0.100 ml g^{-1} and 0.0972 ml g^{-1} respectively in 0.3 M and 1 M NaCl). The water content was determined with the help of Karl Fischer titrations.

(d) Sucrose (BDH aristar). The measurements on sucrose were also extrapolated to infinite dilution, using the same dependence of K' (eq. (1)) on the refractive index of the solution as Maron and Lou [44] did. Contrary to Maron and Lou and Mijnlieff [45] we found no substantial depolarisation ($\rho_u \leqslant 0.01$).

All calibration constants agreed within 1.5%. Comparison of the calibration constants obtained from the aqueous solutions and from benzene leads to the conclusion that the influence of the refractive index of the solution on the calibration constant is much less than the theoretically expected [46–48] n^2 (actually we obtained a value quite close to n). This might partially be caused by the fact that the photomultiplier does see past the incident beam [49].

8.5. Micellar weight determinations

8.5.1. Ultracentrifugation equilibrium

In analysing the data from equilibrium experiments use is made of the interference and the Schlieren pattern. The fringes and the refractive index gradients were converted to concentrations or concentration gradients respectively with the help of eq. (22). We thus ignore the influence of the pressure on the refractive indices and index increments. The reduced total apparent weight average molecular weights at concentrations above the CMC and at different positions in the cell were calculated with the help of a computer program of Ketellapper [50].

* The β-lactoglobulin was a generous gift of Dr. T.A.J. Payens of the Netherlands Institute of Dairy Research, Ede, The Netherlands.

The results for diC_6- and diC_7-lecithin are plotted in figs. 3 and 4. The experiments on diC_7- were very poorely reproducible. This large nonsuperposition of the curves cannot be explained on the basis of the pressure influence on the association equilibrium and is probably due to traces of impurities or to decomposition of the lecithin during the 40 hours centrifugation. When analysing average molecular weights of diC_7- at the meniscus and the bottom of the cell at shorter time intervals (Archibald method) this "decomposition effect" has in fact a few times been observed. The direction of the change of the molecular weights was, however, not always the same. In two experiments a slight increase, while in one other a larger decrease was found. Seven experiments, indicated with dots in fig. 4, show a molecular weight–concentration dependence basically different from the results of the other nine experiments. These deviating lines are curved upwards or have a very pronounced S-shape. Such plots are often obtained in experiments where the sedimentation equilibrium is not reached or in cases where the micellar equilibria are disturbed by impurities.

The measured values of $\langle M\, \partial\rho/\partial c\rangle_{w,app.}$ from all experiments were averaged and a smooth curve was drawn. The standard deviation of the experimental points around this mean curve is 5 to 7%. An other average curve was obtained by excluding the seven experiments marked with dots. The standard deviation now is around 3%.

The resulting mean curves of diC_6- and diC_7- were graphically extrapolated into the CMC region. As a guide in this extrapolation CMC values from surface tension measurements [1] were used. These values are indicated by arrows in figs. 3 and 4. After analysis of the entire curves with the help of eqs. (10) (modified so as to contain apparent quantities), (13) and (21) the apparent *micellar* weight–concentration dependence is obtained. The results are plotted in figs. 5 and 6. The broken lines in fig. 6 from ultracentrifugation were obtained by taking all results from fig. 4 into account. If only the nine more well behaved experiments are used the micellar weights equal the data from light scattering. At micellar concentrations below 4 mg ml^{-1} the micellar weights are dramatically influenced by slight changes in the extrapolation of the total average molecular weight to the monomeric region. By trial and error extrapolations were found that yield acceptable micellar weight against concentration plots. The sudden increase in micellar weight going to very low micelle concentrations

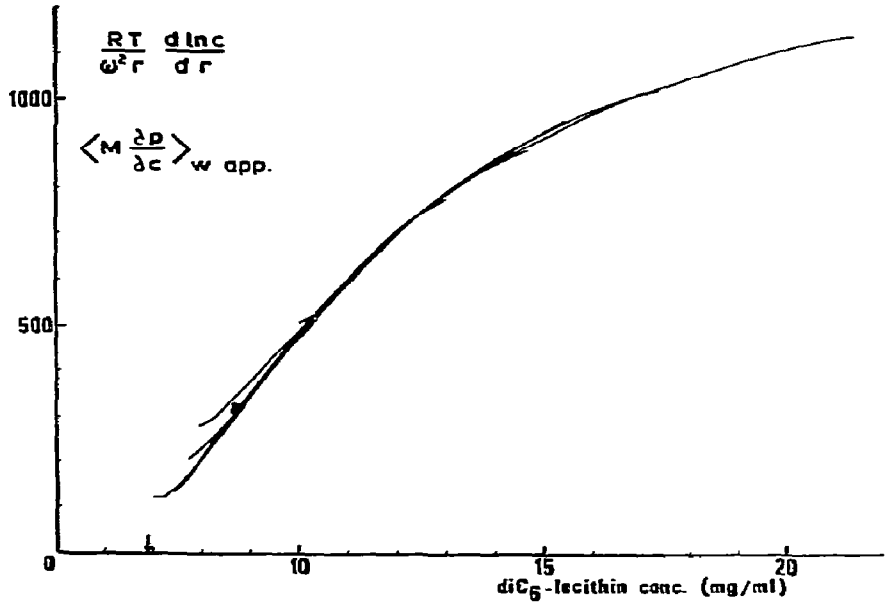

Fig. 3. Results from five ultracentrifugation experiments on diC_6-lecithin in aqueous solutions containing 10^{-2}M phosphate buffer (pH = 6.9 ± 0.1). In this figure and in figs. 4 and 7–10 the arrows indicate the CMC obtained by surface tension measurements [1].

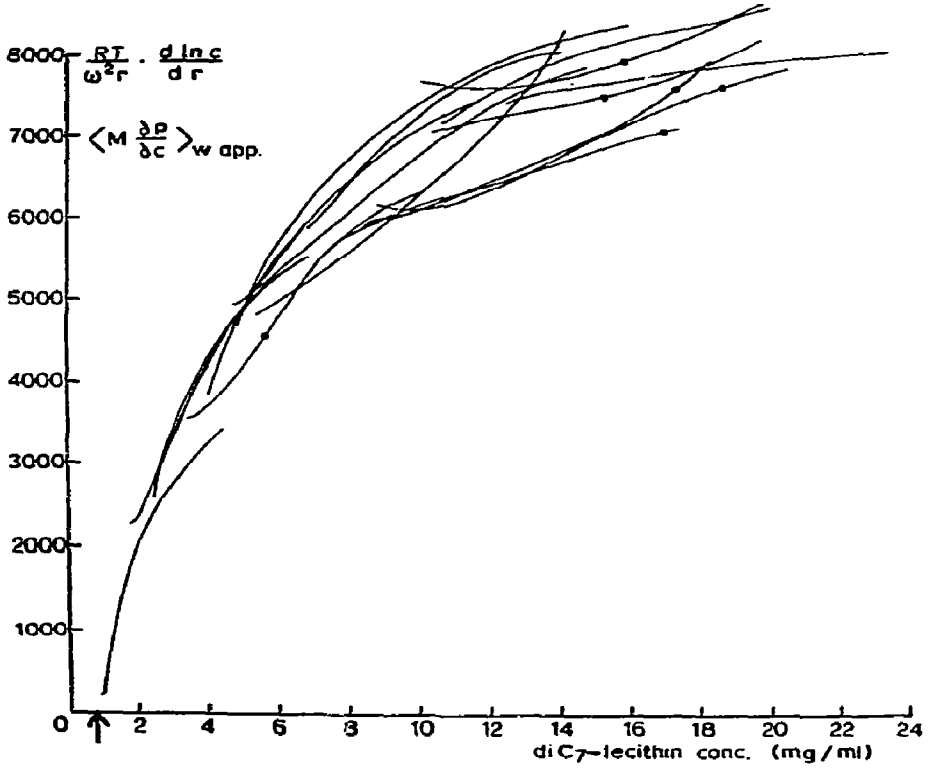

Fig. 4. Results from sixteen ultracentrifugation experiments on diC_7-lecithin in aqueous solutions containing 10^{-2} M phosphate buffer (pH = 6.9 ± 0.1).

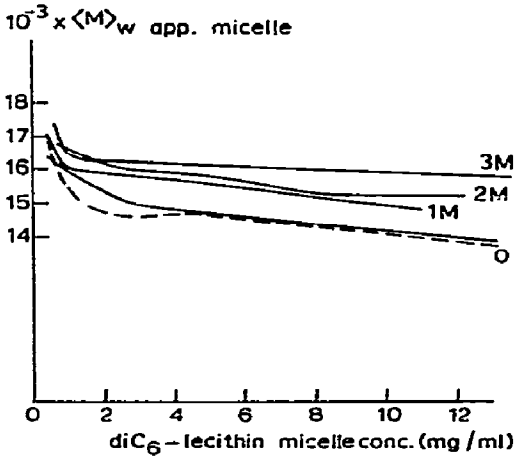

Fig. 5. Apparent weight average micellar weights as a function of the diC_6-micellar lecithin concentration. The broken line is derived from ultracentrifugation experiments (dilute buffer solutions). The fully drawn lines are obtained from light scattering, the solutions contained various NaCl concentrations next to the phosphate buffer.

is caused by mathematical difficulties in the numerical integration in eq. (10) and has no physical significance.

8.5.2. Light scattering

In fig. 7 the R_{90} values for diC_6-lecithin in 0, 1, 2 and 3 M NaCl are shown and in fig. 8 R_{90} for diC_7- in 0 and 3 M NaCl is plotted. Owing to the limited quantity of diC_7-lecithin, we calculated the value for the refractive index increments in 3 M NaCl, with the help of eq. (23): $(\partial n/\partial c)_1 = 0.112$ and $(\partial n/\partial c)_m = 0.101$. This may have introduced systematic errors of a few percent.

The plots of $R_{90}/K'c$ for concentrations above the CMC are shown in figs. 9 and 10. The values for concentrations below the CMC are consistently too high, probably due to some dust. Owing to the limited quantities of the lecithins we used as little material as possible and prepared stock solutions in the light scattering cuvettes. Dilutions were carried out in the cells and by the time the CMC was reached, after three to five dilutions, the dust level was mostly too high (dissymmetry $z \approx 1.03$ to 1.04). The curves were extrapolated to the CMC in a manner completely analogous to the procedure used in analysing the ultracentrifugation data. The apparent micellar weights were obtained with the help of eqs.

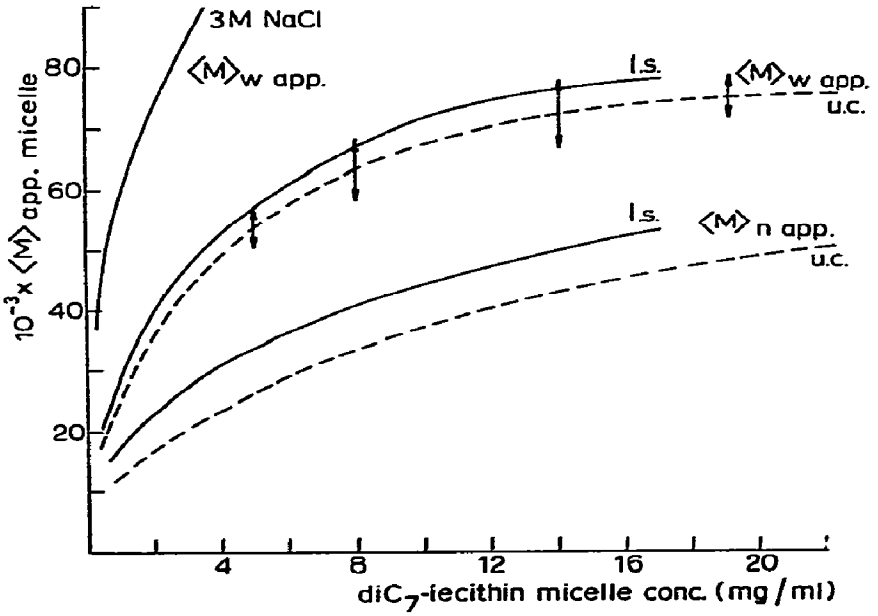

Fig. 6. Apparent weight and number average micellar weights of diC_7-lecithin as derived from light scattering (l.s.——) and ultracentrifugation (u.c. ····). The arrows (↕) indicate the standard deviation of the ultracentrifugation data around the mean values.

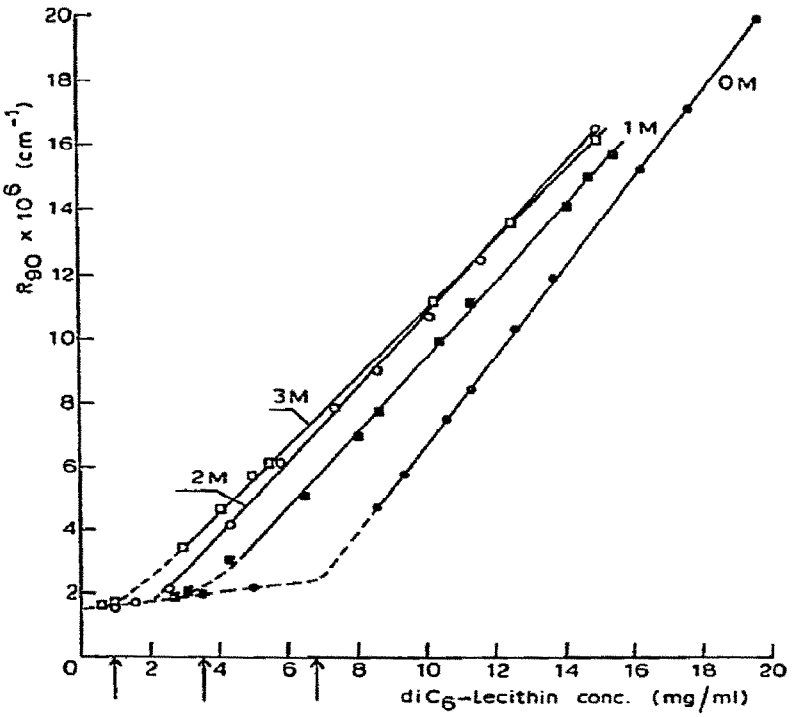

Fig. 7. Rayleigh ratio (R_{90}) as a function the diC$_6$-lecithin concentration in aqueous solutions containing in addition to the phosphate buffer (10^{-2} M, pH = 6.9 ± 0.1) various concentrations of NaCl. (•): 0 M, (▪): 1 M, (○): 2M, (□): 3M NaCl.

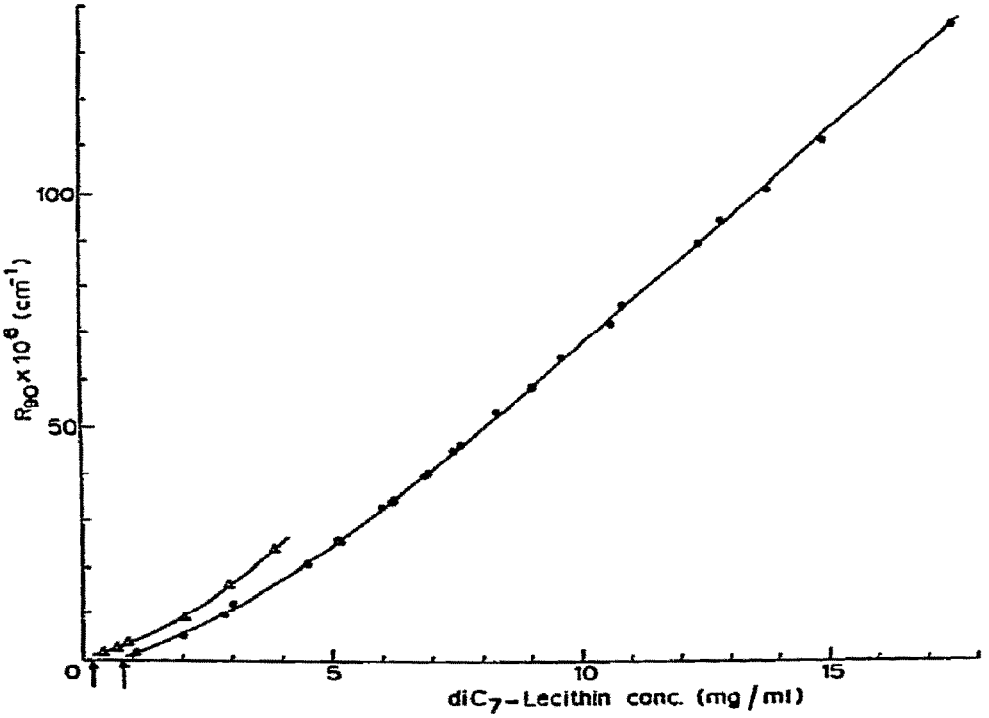

Fig. 8. Rayleigh ratio (R_{90}) as a function of the diC$_7$-lecithin concentration in aqueous buffer solutions containing 0 M (•) and 3M NaCl (△).

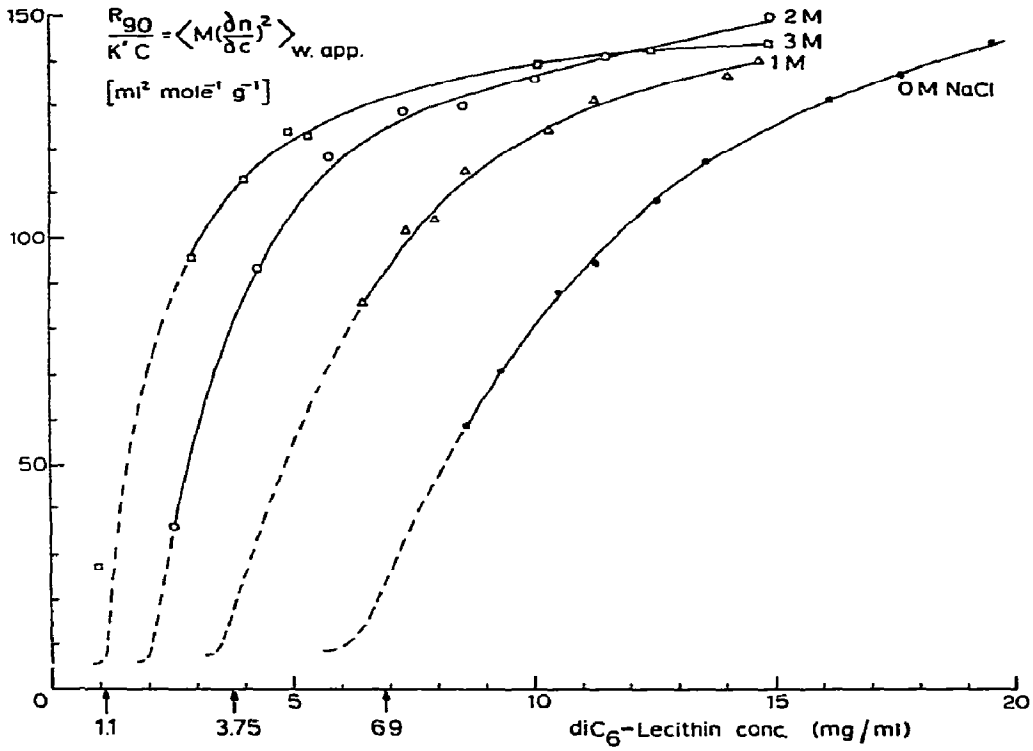

Fig. 9. Reduced apparent total weight average molecular weight of diC_6-lecithin as a function of the lecithin concentration in buffer solutions containing various NaCl concentrations. (•): 0 M, (△): 1 M, (○): 2 M, (□): 3 M NaCl.

(10), (13) and (21) and are also plotted in figs. 5 and 6.

9. Micellar models

9.1. diC_6-Lecithin

The apparent micellar weight of diC_6- (fig. 5) shows a slight decrease with increasing concentrations, due to nonideality. Applying eq. (11) to these apparent micellar weights then leads immediately to $\langle M \rangle_{w,app,mic.} / \langle M \rangle_{n,app,mic.} < 1$. A further analysis is only possible after correction for nonideality. As a first approximation we assume the micelles to be monodisperse. For the shape of the micelles we use two simple and rather extreme models: (I) a compact sphere, in which the whole lecithin molecules are accomodated, (II) a spherocylinder with a pure hydrocarbon center [51]. The length of the molecule depends to a great extent on the unknown orientation of the polar group (see, e.g., Cadenhead et al. [52] and their references). We will use a length, in the radial direction, of the polar part of 8 to 11 Å. This polar part includes the carboxylic groups and the glycerylphosphorylcholine and has a maximal extended length of about 14 Å, as determined from molecular models.

9.1.1. Model I: Compact sphere

From the measured partial specific volume of the lecithin micelles and the micellar weight (≈ 15 000) a radius of 18 Å is found. This value is quite reasonable in view of the length of the monomer. To calculate the excluded volume of the lecithin species we also have to take the hydratation of the polar groups into account [53], with the help of

$$\bar{v}_{\text{fh}} = \bar{v}_i + \delta, \qquad (24)$$

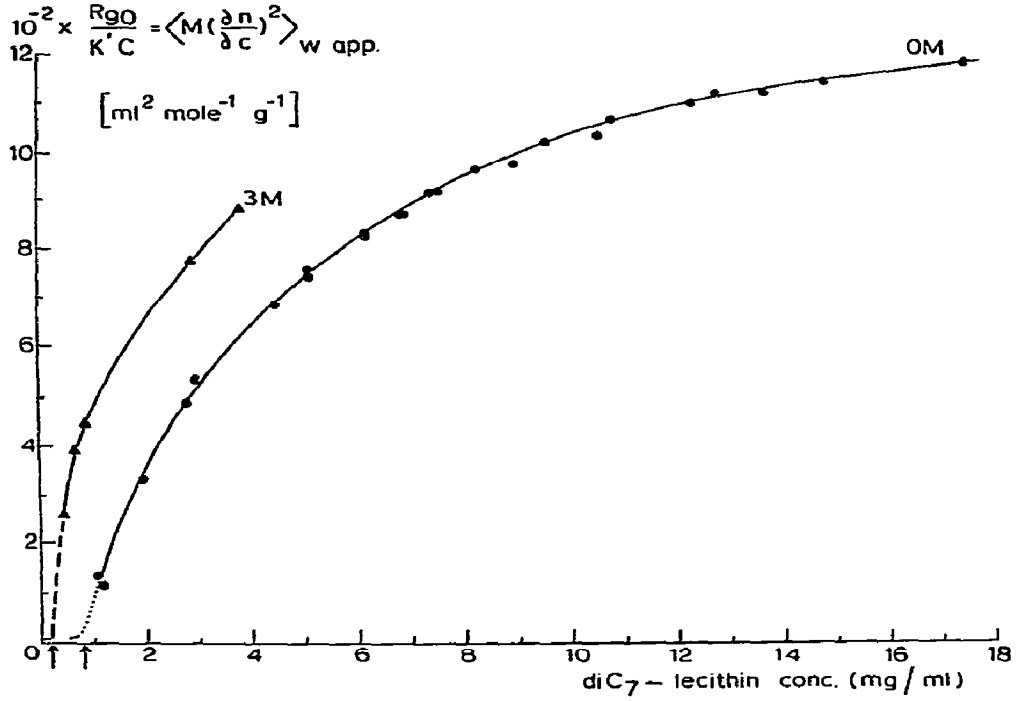

Fig. 10. Reduced apparent total weight average molecular weight of diC_7-lecithin as a function of the lecithin concentration in aqueous buffer solutions containing 0 M (•) and 3 M (▲) NaCl.

where $\bar{v}_{\bar{lh}}$ is the volume per gram hydrated lecithin, $\bar{v}_l$ is the partial specific volume and δ is the hydration in gram water of density 1 per gram lecithin. The literature values of the hydration vary from 7 to 20 water molecules per lecithin molecule, depending on the method used (see, e.g., refs. [54–57] and references quoted therein). A value of 10 water molecules per molecule lecithin seems quite reasonable. The influence of the hydration layer on the calculated values for the ideal micellar weights is small (a few percent at the highest lecithin concentration). Using this model of hydrated spherical monomers and monodisperse micelles the real weight average micellar weights were calculated and plotted in fig. 11.

9.1.2. Model II: Spherocylinders

One can visualise the micelles in an alternative model, where the contact between the hydrocarbon part of the molecules and water and the polar parts is avoided [51]. Using the equations [51] for the hydrocarbon volume v (eq. (25)) and the maximal radius r of the hydrocarbon

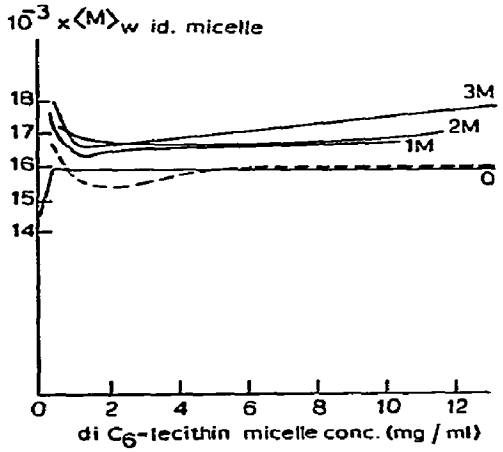

Fig. 11. diC_6-Lecithin ideal micellar weights as a function of the micellar concentrations. The apparent micellar weights are idealised using the compact sphere model (see section 9). The broken line represents ultracentrifugation data, the full lines stem from light scattering.

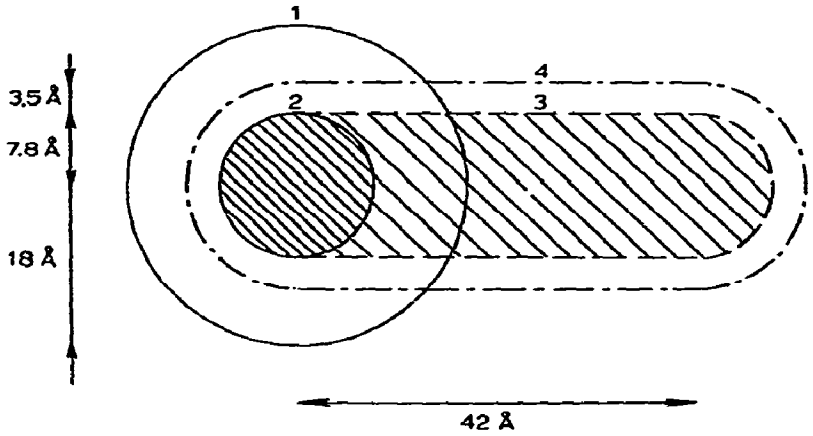

Fig. 12. Section through the diC_6-lecithin micelle model. Circle 1 represents the contour of the compact sphere (radius = 18 Å). Circle 2 is the contour of the hydrocarbon core with radius 7.8 Å and a volume large enough to contain 6.8 monomers. Within the volume surrounded by 3 the hydrocarbon parts of 34 monomers (micellar weights 16 000) can be situated. The volume within 4 is the minimum to contain 34 hydrated lecithin molecules.

core (eq. (26)) one finds that a spherical micelle of diC_6 can accomodate only 6 to 7 monomers.

$$v = 27.4 + 26.9 \times 2 \times n \text{ Å}^3, \quad (25)$$

$$r = 1.5 + 1.265 \times n \text{ Å}, \quad (26)$$

n is the number of carbon atoms per chain participating in the hydrocarbon core (for diC_6: $n = 5$, $v = 296.4$ Å^3, $r = 7.8$ Å). As the micelles however contain about 35 monomers the geometry has to depart from the spherical. For simplicity's sake we introduce the spherocylindrical model. We now have to choose the outer radius R of the spherocylinder. We use two values $R = 15$ Å and $R = 18$ Å. From the molal volume a value for a of 11.2 Å would suffice, but this seems impossible without a great strain on the chemical bonds in the lecithin molecule. The spherocylindrical model is shown in fig. 12 and the calculated ideal micellar weights are shown in figs. 13 and 14.

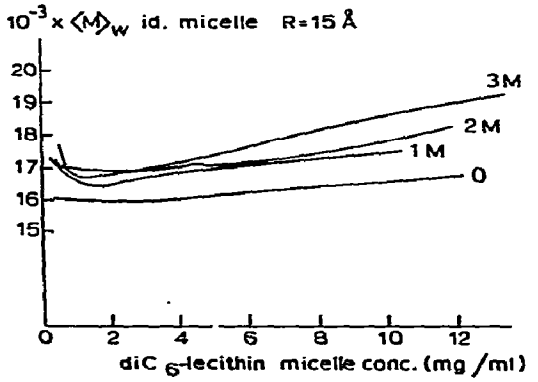

Fig. 13. Weight average micellar weights, from light scattering, as a function of the diC_6-lecithin micellar concentration, in aqueous solutions containing various NaCl concentrations. The micellar weights are corrected for non-ideality using the spherocylinder model (see section 9.1.2) with a radius of 15 A.

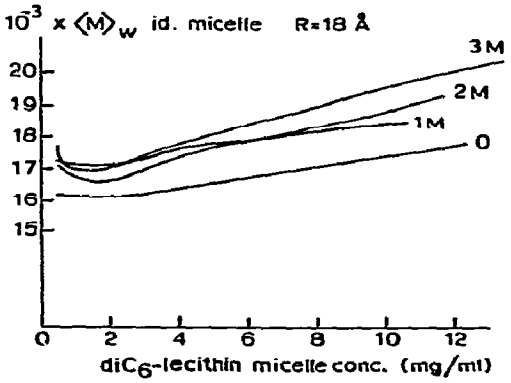

Fig. 14. Same as fig. 13, now for $R = 18$ A.

9.2. diC_7-Lecithin

The apparent micellar weight increases with concentration (fig. 6). This system is clearly polydisperse: $\langle M\rangle_{w.app.mic.}/\langle M\rangle_{n.app.mic.} \approx 1.5$, as calculated with eq. (11). The ratio for the ideal average molecular weights will be higher and we use as a first approximation $\langle M\rangle_{w.id.mic.}/\langle M\rangle_{n.id.mic.} = 2$. This simplifies the Schulz distribution function eq. (18). Again we use two models for estimating the interaction parameter A_{ij}.

9.2.1. Model I

In analogy to the compact sphere of diC_6-lecithin we assume the maximal compact sphere of diC_7-lecithin micelles to have a radius of 19 Å. These micelles can accommodate about 40 monomers ($\langle M\rangle_{w.mic.} \approx 20\,000$). As the micelles grow far beyond this value, we assume the larger micelles to be spherocylinders with radii of 19 Å and different lengths. Again a hydration of 10 water molecules per lecithin molecule is added. We also assume spherical micelles with association numbers between 2 and 40 to be present. This last assumption has a very minor effect on the second virial coefficients. The calculated ideal weight average micellar weights are shown in fig. 15.

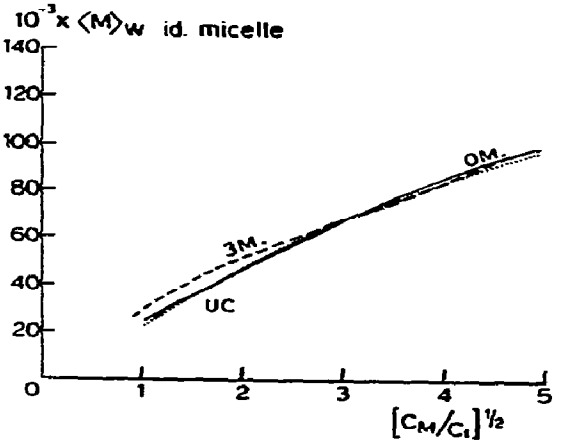

Fig. 16. Ideal weight average micellar weights of diC_7-lecithin as a function of the root of the ratio of micellar and monomer concentration. The molecular weights are idealised using the compact micelle model (see section 9.2.1). The dotted line (····) is derived from ultracentrifugation (only buffer present). The full line (——) and the broken line (– – – –) were obtained from light scattering in 0 M and 3 M NaCl respectively.

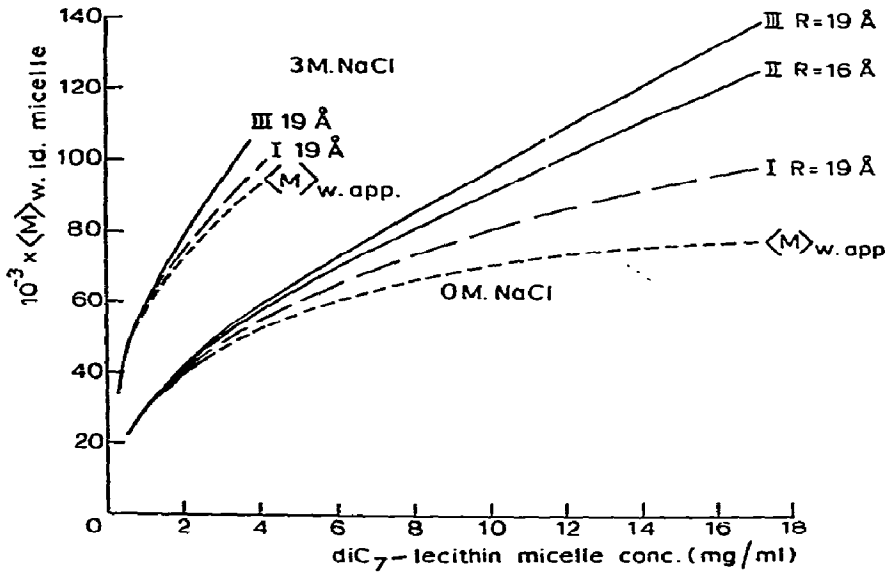

Fig. 15. Weight average micellar weights of diC_7-lecithin as a function of the micellar concentration. In 0 M and 3 M NaCl (upper set of curves). The dotted lines represent the apparent weights. The broken lines I are obtained from the compact micelle model (type I) and the full drawn lines II and III are derived from the spherocylinder model (type II) with radii of 16 Å and 19 Å respectively and with as little hydrocarbon–water contact as possible.

9.2.2. Model II

Avoiding the hydrocarbon–water contact in spherocylinders with hydrocarbon core radii of 9.1 Å leads to much longer micelles and greater second virial coefficients. In analogy to the diC_6-micelle we assume an outer radius of 16 Å and 19 Å. Results for the ideal molecular weights are shown in fig. 16.

10. Discussion

10.1. Micellar weights

In analysing micellar weights the association model is seldom used, partly due to the complication of the slight increase of the monomer concentration at total concentrations above the CMC. Usually micellar weights are evaluated with the assumption of a constant monomer concentration, for example in the so called Debye-plot [58] in light scattering $H(c - \mathrm{CMC})/(\tau - \tau_{\mathrm{CMC}})$ versus $c - \mathrm{CMC}$. This last method does give accurate results at high micellar concentrations in respect to the CMC.

The results of diC_6-lecithin, where the CMC is relatively high, are, however, significantly different when calculated by both methods, as can be seen from table 4. The second virial coefficients given there are calculated from the apparent micellar weights (fig. 5) with the help of the relation

$$\langle M\rangle^{-1}_{\mathrm{w.id.mic.}} = \langle M\rangle^{-1}_{\mathrm{w.app.mic.}} + 2Bc_{\mathrm{mic.}} \qquad (27)$$

Table 4

Micellar weights of dihexanoyllecithin in aqueous solutions containing various NaCl concentrations

NaCl conc. (M)	$\langle M_w(c_{\mathrm{mic.}} \to 0)$ Debye-plot	$\langle M_w(c_{\mathrm{mic.}} \to 0)$ Association model	Virial coeff. $2B \times 10^4$ (mole ml g^{-2}) Association model
0	13200	15400	5.7 ± 0.1
1	14100	16200	5.0 ± 0.2
2	14700	16350	4.7 ± 0.3
3	15500	16300	1.6 ± 0.1

In this equation $\langle M\rangle_{\mathrm{w.id.mic.}}$ equals the micellar weight, linearly extrapolated to micellar concentration zero. In this case the weight average loses its significance, since calculating the virial coefficient in this manner implies a monodisperse system. Analysis from the Debye-plots reveals no significant virial coefficient ($2B < 10^{-5}$ mole ml g^{-2}), because the plots of the turbidities versus the total concentrations are straight lines (fig. 7). This situation is also found in other micellar systems, especially with nonionic or zwitter-ionic surfactants [59–61].

DiC_7-lecithin gives Debye-plots with a negative virial term, which implies a polydisperse system.

It is essential to have a model for calculating the second virial coefficients. In this article we have used the simplest possible model: an excluded volume based on rigid noninteracting particles. The geometric models for the micelles have been discussed in detail in section 9. Our simplified approach does seem to give answers in the right order of magnitude as can be seen from the diC_6-lecithin results (figs. 5, 11, 13, 14) where the decrease in the apparent molecular weight completely disappears upon idealising the molecular weights.

From the graphs we may conclude that the *diC_6-lecithin* micelles have rather narrow weight distributions, at least compared to the diC_7-micelles (to be discussed below). An impression of the width of the distribution can also be obtained from the ratio $Q = \langle M\rangle_{\mathrm{w.id.mic.}}/\langle M\rangle_{\mathrm{n.id.mic.}}$, as has been discussed in section 5. The lowest significant value for Q that can be obtained with our experimental methods is around 1.04. The highest values for Q are obtained for the spherocylinder (model II) with a radius of 18 Å: at a total concentration of 19 mg ml^{-1} (micellar concentration = 12 mg ml^{-1}) we obtain $Q = 1.06$ for the NaCl free solutions and $Q = 1.1$ in the presence of 3 M NaCl.

diC_7-Lecithin micelles are clearly very polydisperse with Q values around 2 (see figs. 6, 15). Using the spherocylinder (model II) with little hydrocarbon–water contact and radii of 16 Å and 19 Å we find at a total concentration of 16 mg ml^{-1} (micellar concentration = 15.2 mg ml^{-1}) $Q = 2.1$ and $Q = 2.0$ respectively. For the more compact and shorter micelles (model I) we find $Q = 1.7$. As pointed out previously (section 5) these wide distributions are obtained if all association constants leading to different types of micelles are about equal. The micellar weight is then proportional to the square root of the micellar concentration. In figs. 16 and 17

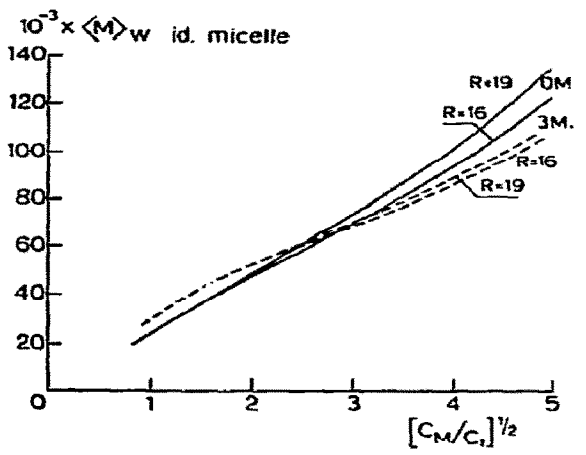

Fig. 17. Idealised weight average micellar weight of diC_7-lecithin from light scattering. The full lines are derived from NaCl free and the broken lines from aqueous solutions containing 3 M NaCl. Two different radii of the spherocylinders (R = 16 Å and R = 19 Å) with as little hydrocarbon–water contact as possible are used (see section 9.2.2).

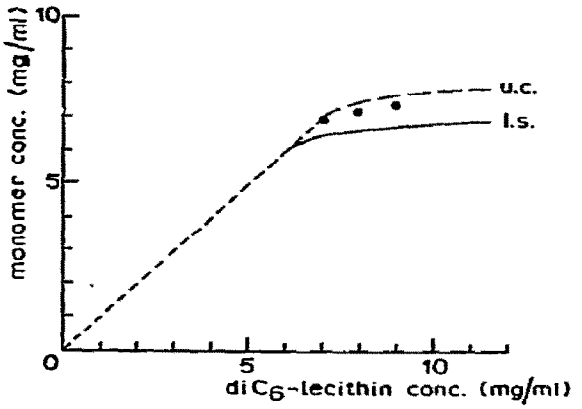

Fig. 18. The monomer concentration of diC_6-lecithin as a function of the total lecithin concentration. The full line is calculated from light scattering, the broken line from ultracentrifugation. The three dots were obtained from surface tension measurements [1].

we have plotted the ideal micellar weights calculated from our different models against $(C_{mic.}/C_{mon.})^{1/2}$.

The results of the experiments performed in 3 M NaCl, where micellar weights increase much more steeply with the micellar concentration than in 0 M NaCl (figs. 13 and 14) are now very close to the data obtained in NaCl free solutions. This could mean that all association constants increase in the same way with increasing salt concentrations, by a kind of salting-out mechanism [1, 62].

10.2. Monomer concentration of diC_6-lecithin

Although the micellar weights obtained from light scattering and ultracentrifugation agree very well with each other the monomer concentrations differ significantly. The calculated results are shown in fig. 18. The CMC obtained from ultracentrifugation is 7.0 mg ml^{-1} and is in fair agreement with the CMC as obtained from surface tension measurements [1] (6.9 mg ml^{-1}). Light scattering gives a CMC of 6.2 mg ml^{-1}. The three points in fig. 18 have been calculated from surface tension measurements [1] by extrapolation of the linear part of the γ versus log c curve below the CMC. To explain the differences between these data several hypotheses can be proposed in connection with the presence of dust in light scattering or decomposition of the lecithin in centrifugation experiments, but no definite opinion can yet be given.

If the monomer concentration as a function of the total concentration is accurately known micellar weights can be estimated. We made some calculations for diC_6-lecithin in 3 M NaCl using the surface tension data [1] and the monodispers micellar model with no thermodynamic nonideality. After curve fitting a micellar weight of 17 000 ± 1 000 was obtained, which is in remarkable agreement with the light scattering data.

11. Conclusion

The association of dihexanoyllecithin leads to the formation of micelles with an apparent measured micellar weight of about 15 000 to 14 000 in solutions of low electrolyte content (fig. 5). The slight decrease of these values with increasing lipid concentration completely disappears after introduction of a thermodynamic nonideality correction based on the excluded volume of the lecithin. The micellar weights corrected for this effect range from 16 000 to 17 500 (figs. 11, 13 and 14). A rather narrow size distribution is observed. The results are rather insensitive to the details in the numerical assumptions involved in the analysis. Roholt and

Schlamowits [63] obtained a somewhat larger micellar weight.

Diheptanoyllecithin, however, associates into much larger aggregates with wide weight distributions. The apparent micellar weights range from 20 000 to 80 000 (fig. 6). The influences of the assumptions, concerning the geometric model of the micelles, on the nonideality correction are much greater than in the case of the shorter homologue (figs. 15, 17). Smink [64] reported a micellar weight of 30 000. He, however, gives no further details and we presume that he calculated this molecular weight after extrapolation to infinite dilution.

Addition of NaCl to the dihexanoyl compound has only a very limited effect on the micellar weight (fig. 5). It therefore seems fair to conclude that the electrostatic zwitterionic dipole interactions are of minor importance to the lecithin micellar size in a monodisperse system. The large increase in the association number of the higher homologue on addition of NaCl (fig. 15) is expected if all association constants from this multiple equilibrium system are increased, for instance by a salting out mechanism, which also explains the strong decrease of the CMC.

Acknowledgements

The authors are indebted to Mr. L.W. Ketellapper for the many helpful suggestions and discussions and to Miss J.C. Hopman for her skilful assistance in the ultracentrifugation experiments. We would also like to thank Mr. A.A. Caljé for his useful contribution with vapor pressure osmometry. The authors are indebted to Dr. H.A.M.G. Vaessen of the National Institute of Public Health, Laboratory for Chemical Analysis of Foodstuffs, Bilthoven, and to Miss T.A. Schippers of the Pharmaceutical Laboratories, Utrecht, for their Karl Fischer titrations on tungstosilicic acid.

References

[1] R.J.M. Tausk, J. Karmiggelt, C. Oudshoorn and J.Th.G. Overbeek, Biophys. Chem. 1 (1974) 175.
[2] H.G. de Haas, P.P.M. Bonsen, W.A. Pieterson and L.L.M. van Deenen, Biochim. Biophys. Acta 239 (1971) 252.
[3] K.E. van Holde, Fractions 1 (1967), Beckman Instruments Inc.
[4] J.A. Brinkhuis, H.J. Vreeman and L.W. Ketellapper, J. Electroanal. Chem. 37 (1972) 343.
[5] H.F. Huisman, Koninkl. Ned. Akad. Wetensch. Proc. Ser. B 67 (1964) 367.
[6] O. Kratky, H. Leopold and H. Stabinger, Z. Angew. Physik 27 (1969) 273.
[7] L.J. Gostings, J. Am. Chem. Soc. 72 (1950) 4418.
[8] H. Yamakawa, Modern theory of polymer solutions, Harper & Row, New York, 1971 ch. 5.
[9] W.H. Stockmayer, J. Chem. Phys. 18 (1950) 58.
[10] T.L. Hill, Statistical mechanics (McGraw-Hill, New York, 1956).
[11] T.L. Hill, J. Chem. Phys. 30 (1959) 93.
[12] E.F. Cassasa and H. Eisenberg, Advan. Protein Chem. 19 (1964) 287.
[13] H. Fujita, Mathematical theory of sedimentation analysis, eds. E. Hutchinson and P. van Rysselberghe (Academic Press, New York, 1962).
[14] E.T. Adams and J.W. Williams, J. Am. Chem. Soc. 86 (1964) 3454.
[15] E.T. Adams and D.L. Filmer, Biochemistry 5 (1966) 2971.
[16] J.M. Corkill, J.F. Goodman, T. Walker and J. Wyer, Proc. Roy. Soc. A 312 (1969) 243.
[17] J.M. Corkill and J.F. Goodman, Advan. Coll. Interf. Sci. 2 (1969) 297.
[18] P. Mukerjee, J. Phys. Chem. 76 (1972) 565.
[19] B.H. Zimm, J. Chem. Phys. 14 (1946) 164.
[20] C. Tanford, Physical chemistry of macromolecules (Wiley, New York, 1965) p. 196.
[21] H. Reerink, J. Colloid. Sci. 20 (1965) 217.
[22] H.G. Elias, R. Bareiss and J.G. Watterson, Advan. Polymer Sci. 11 (1973) 111.
[23] G. Herdan, Nature 163 (1949) 139.
[24] J.G. Watterson and H.G. Elias, Kolloid Z.Z. Polym. 249 (1971) 1136.
[25] J.M. Corkill, K.W. Gemmel, J.F. Goodman and T. Walker, Trans. Faraday Soc. 66 (1970) 1274.
[26] G.V. Schulz, Z. Phys. Chem. B 47 (1940) 155.
[27] A. Isihara, J. Chem. Phys. 18 (1950) 1446.
[28] A. Isihara, J. Chem. Phys. 19 (1951) 397.
[29] A. Isihara, J. Phys. Soc. Japan 6 (1951) 40.
[30] A. Isihara, J. Phys. Soc. Japan 6 (1951) 46.
[31] T. Kihara, J. Phys. Soc. Japan 8 (1953) 686.
[32] G.J. Howlett, P.D. Jeffrey and L.W. Nichol, J. Phys. Chem. 76 (1972) 777.
[33] W. Heller, Rec. Chem. Progr. 20 (1959) 209.
[34] J.M. Corkill, J.F. Goodman and T. Walker, Trans. Faraday Soc. 63 (1967) 768.
[35] F.C. Reman, Thesis, Utrecht (1971).
[36] T. Gulik–Krzywicki, E. Rivas and V. Luzzati, J. Mol. Biol. 27 (1967) 303.
[37] V. Luzzati, T. Gulik–Krzywicki and A. Tardieu, Nature 218 (1968) 1031.
[38] M.R. Bruzzesi, E. Chiancone and E. Antonini, Biochemistry 4 (1965) 1796.
[39] R.C. Deonier and J.W. Williams, Biochemistry 9 (1970) 4260.
[40] R.E. Canfield, J. Biol. Chem. 238 (1963) 2698.
[41] J. Visser, R.C. Deonier, E.T. Adams and J.W. Williams, Biochemistry 11 (1972) 2634.

[42] M. Halwer, G.C. Nutting and B.A. Brice, J. Am. Chem. Soc. 73 (1951) 2786.
[43] J.P. Kratohvil, L.E. Oppenheimer and M. Kerker, J. Phys. Chem. 70 (1966) 2834.
[44] S.H. Maron and R.L.H. Lou, J. Phys. Chem. 59 (1955) 231.
[45] P.F. Mijnlieff, H. Zeldenrust, J. Phys. Chem. 69 (1965) 689.
[46] J.J. Hermans and S. Levineson, J. Opt. Soc. Am. 41 (1951) 460.
[47] D.J. Coumou, J. Colloid. Sci. 15 (1960) 408.
[48] E. Ahad and B.R. Jennings, J. Phys. D3 (1970) 1509.
[49] H.J. Cantow, J.U.P.C., Intern Symp. Macromol. Chem. p. 504, Milano, Torino (1954).
[50] L.W. Ketellapper, to be published.
[51] C. Tanford, J. Phys. Chem. 76 (1972) 3020.
[52] D.A. Cadenhead, R.J. Damchak and M.C. Phillips, Kolloid Z.Z. Polym. 220 (1967) 59.
[53] C. Tanford, Physical chemistry of macromolecules (Wiley, New York, 1965) p. 339.
[54] D.M. Small, J. Lipid Res. 8 (1967) 551.
[55] W.V. Walten and R.G. Hayes, Biochim Biophys. Acta 249 (1971) 528.
[56] C. Horwitz, L. Krut and L.S. Kaminsky, Chem. Phys. Lipids 8 (1972) 185.
[57] J.L. Rigaud, Y. Lange, C.M. Carry–Bobo, A. Samson and M. Ptak, Biochem. Biophys. Res. Commun. 50 (1973) 59.
[58] P. Debye, Ann. N.Y. Acad. Sci. 51 (1949) 575.
[59] K.W. Herrmann, J. Coll. Interf. Sci. 22 (1966) 352.
[60] J.B. Daruwala, Thesis, Connecticut (1969).
[61] J. Swarbrick and J.B. Daruwala, J. Phys. Chem. 74 (1970) 1293.
[62] P. Mukerjee, J. Phys. Chem. 69 (1965) 4038.
[63] O.A. Roholt and M. Schlamowitz, Arch. Biochem. Biophys. 94 (1961) 364.
[64] D.A. Smink, Thesis, Leiden (1969).